Chaos, Solitons and Fractals 155 (2022) 111720

Contents lists available at ScienceDirect

Chaos, Solitons and Fractals

Nonlinear Science, and Nonequilibrium and Complex Phenomena

journal homepage: www.elsevier.com/locate/chaos

Correlation lags give early warning signals of approaching bifurcations

Giulio Tirabassi, Cristina Masoller*

Departament de Fisica, Universitat Politecnica de Catalunya, Barcelona, Spain

ARTICLE INFO

Article history:
Received 17 November 2021
Accepted 9 December 2021
Available online 30 December 2021

Keywords:
Bifurcations
Early warning signals
Critical slowing down
Tipping points

ABSTRACT

Identifying approaching bifurcations and regime transitions from observations is an important challenge in time series analysis with practical applications in many fields of science. Well-known indicators are the increase in spatial and temporal correlations. However, the performance of these indicators depends on the system under study and on the type of approaching bifurcation, and no indicator provides a reliable warning for any system and bifurcation. Here we propose an indicator that simultaneously takes into account information about spatial and temporal correlations. By performing a bivariate correlation analysis of signals recorded in pairs of adjacent spatial points, and analyzing the distribution of lag times that maximize the cross-correlation, we find that the variance of the lag distribution displays an extreme value that is a consistent early warning indicator of the approaching bifurcation. We demonstrate the reliability of this indicator using different types of models that present different types of bifurcations, including local bifurcations (transcritical, saddle-node, supercritical and subcritical Hopf), and global bifurcations.

1. Introduction

Dynamical systems often display regime transitions that can be reversible or irreversible, safe or catastrophic, and may unfold slowly or explosively [1–5]. In the human body, transitions to critical conditions such depression, arrhythmia or epilepsy may occur with no warning. In the Earth system, examples of regime transitions include ice ages, desertifications, population extinctions and epidemic outbreaks, to name just a few. A regime transition may be difficult to recognize, to reverse, to manage, and may trigger a cascade of transitions in inter-dependent subsystems [6–13].

Regime transition are often traced back to the presence of a time-varying parameter and a bifurcation that destroys a stable solution (fixed point, limit cycle, or attractor) or changes its stability, and may generate new solutions [14].

A lot of efforts have focused on identifying "early warning signals" that anticipate an approaching bifurcation or tipping point (where a transition to a new state occurs), directly from data [15–28]. Also efforts have been devoted to understand the mechanisms underlying regime transitions and bifurcations by using experimental "toy models". For example, the study of the light emitted by a laser with a time-varying parameter has shown how the tipping point (when the laser turns on) depends on the rate of variation of the control parameter, the level of noise, and the initial conditions [29,30]. The experimentally recorded optical signals have also been used to test early warning indicators [31,32].

An indication of an approaching bifurcation is known as "Critical Slowing Down" (CSD): as the system approaches the bifurcation point, the dynamics becomes slower, and the relaxation time to equilibrium increases. Since the dynamic slows down, the autocorrelation of the observed variable increases. The slowdown is quantified by the lag-1 autocorrelation of the observed variable, and may also lead to an increase in its variance. In the presence of spatial diffusion, as a bifurcation is approached the spatial correlation may increase, which provides another way to detect CSD from the analysis of the system in different locations [33–37].

However, CSD and significant changes in variance, autocorrelation, or other indicators may fail to predict regime transitions, may raise false alarms, may reveal only particular types of transitions, and may occur only after the tipping point is crossed [32,38–41].

Here we propose to integrate the increase in temporal correlation and the increase in spatial correlation, into a single quantity: the standard deviation, σ_τ, of the distribution of minimum lags, τ_{ij}, that maximize the correlation between time series of an observed variable, u, in neighboring points, $u_i(t) = u(x_i, t)$ and

* Corresponding author.
E-mail address: cristina.masoller@upc.edu (C. Masoller).

https://doi.org/10.1016/j.chaos.2021.111720

$u_j(t) = u(x_j, t)$. We show that this new indicator provides a reliable warning of different bifurcations that occur in different systems, and we propose a simple model that allows us to understand why σ_τ is successful. We also compare the performance of σ_τ with that of two classical indicators, the spatial correlation and the lag-1 autocorrelation.

This paper is organized as follows. In Section 2 we introduce the formal definition of the variance of the lag distribution, σ_τ, and of other two indicators, the lag-1 autocorrelation and the spatial correlation; Section 3 presents the models used to test the performance of these indicators. Section 4 presents the results obtained and Section 5 presents a summary and our conclusions.

2. Early warning indicators

2.1. Variance of the lag distribution

We define the lag, τ_{ij}, that maximizes the correlation between two time series, u_i and u_j, of length N, normalized to have zero mean and unitary variance, as

$$\tau_{ij} = \underset{1\le\tau\le\tau_{\max}}{\text{argmax}_\tau}\left(\left|\sum_{t=1}^{N-\tau_{\max}} u_i(t)u_j(t+\tau)\right|\right). \quad (1)$$

We note that $\sum_t u_i(t)u_j(t+\tau)$ is the Pearson correlation coefficient that is a measure of linear correlation between $u_i(t)$ and $u_j(t+\tau)$.

The variance of the distribution of lags that maximize the correlation is

$$\sigma_\tau = (1/M)\sum_{i,j}(\tau_{ij} - \langle\tau\rangle)^2, \quad (2)$$

where M is the number of (i, j) pairs and $\langle\tau\rangle$ is the average lag, $\langle\tau\rangle = (1/M)\sum_{i,j}\tau_{ij}$.

From an operational point of view, we search for the lag that maximizes the correlation in the interval $[1,\tau_{\max}]$. We start with a minimum lag of 1 (instead of 0) because in the distribution of τ_{ij} values, 0 tends to be overpopulated, regardless of the value of the bifurcation parameter. On the other hand, searching for the maximum in an interval of values provides information about longer time scales than lag-1 cross-correlation. Unless otherwise stated, $\tau_{\max}$ is 4% of the length of the time series. $\tau_{\max}$ is the only free parameter and the sensitivity of σ_τ to the value of $\tau_{\max}$ is analyzed in Section 4.

In Eqs. (1) and (2) the pairs (i, j) are limited to first neighbors in the regular grid of points used to observe the system's dynamics. This choice has two reasons: (i) due to diffusion, every point in the lattice is directly coupled to its first neighbors and (ii) it is computationally efficient as it strongly reduces the number of calculations. We have verified that taking into account higher order neighbors does not improve the performance of the metric. We have also used, instead of the Pearson coefficient, a nonlinear correlation measure (the mutual information, which is computationally more demanding) and found a similar performance of σ_τ.

2.2. Other early warning indicators

To demonstrate the performance of σ_τ, in Section 4 we compare it with the performance of two well-known indicators, the average lag-1 autocorrelation and the average spatial cross-correlation, formally defined as

$$\text{lag-1 CC} = \langle|\langle u_i(t)u_i(t+1)\rangle_t|\rangle_i, \quad (3)$$

$$\text{Spatial CC} = \left\langle\left|\left\langle u_i(t)u_j(t)\right\rangle_{i,j}\right|\right\rangle_t. \quad (4)$$

For the calculation of the spatial correlation, the pairs (i, j) are also limited to first-order neighbors.

Table 1
Parameters used in the simulations of the FHN model.

Bifurcation	Λ	Σ	ν	σ_u	σ_v	D_u	D_v
Saddle-Focus	2	1	1	0.005	0.005	0.5	0.5
Subcritical Hopf	3	2	0.1	0.0001	0.0001	0.001	0.001
Supercritical Hopf	0.3	2	0.1	0.001	0.001	0.005	0.005
Travelling waves	3	2	0.1	0.001	0.001	0.2	0.02

3. Models

To demonstrate the performance of σ_τ we simulate three models where different types of bifurcations occur.

3.1. Scalar bistable 1D model

This model describes a stochastic bistable system defined by a scalar field, $u(x, t)$, in a one-dimensional space [42],

$$\frac{\partial u}{\partial t} = -u^3 - \alpha u^2 + u(1+\alpha) + D\frac{\partial^2 u}{\partial x^2} + \xi. \quad (5)$$

Here α is a control parameter, D is the diffusion coefficient, and ξ is a Gaussian noise term having zero mean and σ^2 variance. The system presents three homogeneous steady-state solutions: $u = 0$, $u = -1 - \alpha$ and $u = 1$. When $\alpha = -1$ or $\alpha = -2$, two solutions collide and exchange stability due to transcritical bifurcations.

3.2. Local positive feedback (LPF) model

This model describes the interaction between biomass B and soil water w in a two-dimensional region [33,36],

$$\frac{\partial w}{\partial t} = R - \frac{w}{\tau_w} - \Lambda w B + D\Delta w + \xi_w,$$
$$\frac{\partial B}{\partial t} = \rho B\left(\frac{w}{w_0} - \frac{B}{B_C}\right) - \mu\frac{B}{B+B_O} + D\Delta B + \xi_B. \quad (6)$$

Here τ_w, μ, ρ, Λ, w_0, B_O, B_C are constant parameters, R is the bifurcation parameter that represents the amount of rainfall, D is the diffusion coefficient, and ξ_B and ξ_w are Gaussian noise terms having zero mean and σ_B^2 and σ_w^2 variance respectively. The simulations were carried out with the same parameter values as in Tirabassi et al. [36]. The observed variable for calculating the early warning indicators was the biomass, B.

3.3. Fitzhugh–Nagumo (FHN) model

This model represents a set of diffusely coupled neurons in a two-dimensional region, forced by an external stimulus, I [43–45]. The model describes the evolution of the membrane potential, u, and the recovery variable, v. The equations read [45]:

$$\frac{\partial u}{\partial t} = \Lambda u - u^3 - \Sigma v - I + D_u\Delta u + \xi_u,$$
$$\frac{\partial v}{\partial t} = \nu(u - v) + D_v\Delta v + \xi_v. \quad (7)$$

Here Λ, Σ and ν are constants, I is taken as bifurcation parameter, D_u and D_v are diffusion coefficients, and ξ_u and ξ_v are Gaussian noise terms having zero mean and variance σ_u^2 and σ_v^2 respectively. The simulations were carried out with the parameter values listed in Table 1. The observed variable for calculating the early warning indicators was the membrane potential, u.

3.4. Model simulations

The models were simulated using the Euler–Maruyama method over a linear periodic grid of 100 points (for the scalar bistable

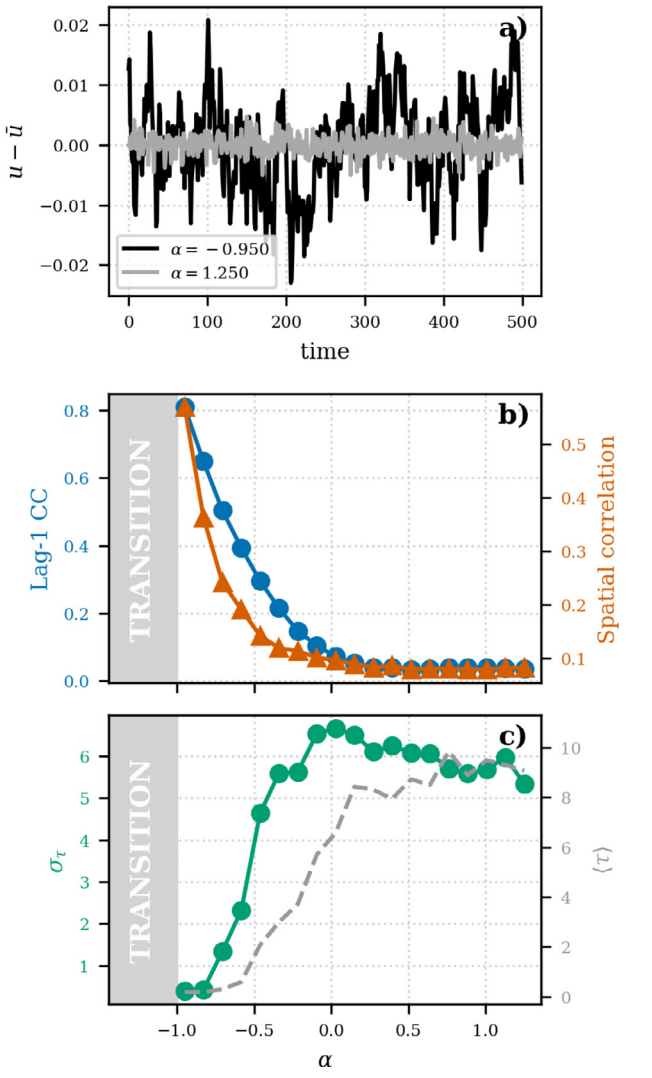

Fig. 1. (a) Dynamics of the scalar bistable 1D model close (black) and far (grey) from the bifurcation at the same spatial location. The parameters $D = 0.2$ and $\sigma = 0.005$. The effect of critical slowing down is evident in the variances of the two time series, with the former being significantly higher than the latter. (b) Conventional early warning indicators, lag-1 temporal correlation and spatial cross-correlation, as a function of the bifurcation parameter, α. (c) Mean, $\langle\tau\rangle$, and standard deviation, σ_τ, of the distribution of lags that maximize the absolute value of the cross-correlation.

1D model) or over a 100 × 100 periodic square lattice (for the LFP and FHN models). The diffusion term was approximated using finite differences $(D\partial^2 u/\partial x^2|_{x=x_i} = D[u(x_{i+1}) + u(x_{i-1}) - 2\,u(x_i)])$. The integration steps were $dt = 0.1$ and $dx = \sqrt{2}/2$ ($dx = 1/2$) for the 1D model (for the 2D models).

Unless otherwise specifically stated, the bifurcation parameter was increased in steps up to the bifurcation point, using the last condition of one simulation as the starting condition of the next simulations. For each value of the bifurcation parameter the time series of the observed variable was recorded in each spatial grid point, every time unit for 1000 time units, after disregarding the first 500 time units to let transients die away.

In a realistic scenario the control parameter varies continuously in time, and we show in the next section that if the parameter variation is slow enough, σ_τ still provides a reliable indication of the approaching bifurcation.

4. Results

In this section we investigate time series obtained by simulating the models presented in the previous section. By studying how σ_τ varies when the control parameter approaches the bifurcation point, we show that σ_τ is more informative than the two other indicators, the lag-1 autocorrelation and the spatial cross-correlation.

4.1. Transcritical bifurcation

We begin by considering the scalar bistable 1D Model presented in Section 3.1. In this model, when α approaches a critical value, two fixed points collide giving rise to a *transcritical bifurcation*. Approaching the bifurcation point, the time series variance increases (Fig. 1a) and CSD is detected through lag-1 correlation and spatial correlation (Fig. 1b). However, although both these quantities increase, their behavior does not reveal how close the system is to the bifurcation, since they grow monotonically and the bifurcation occurs way before they reach their maximum possible value. In contrast, the standard deviation of the distribution of lags, σ_τ, displays a non-monotonic behavior with respect to the bifurcation parameter (Fig. 1c). In particular, approaching the bifurcation σ_τ slightly increases before collapsing, right before the bifurcation point. In Fig. 1c we also note that variation of σ_τ is more informative than the variation of the average lag, $\langle\tau\rangle$, that does not reach a maximum before the bifurcation (dashed line).

4.2. Simple model for estimating σ_τ

The variation of σ_τ can be understood by examining how the distribution of τ_{ij} values changes when the bifurcation is approached. Fig. 2 displays in color code the histograms of τ_{ij} values as a function of α. When α approaches the critical value, τ_{ij} values migrate uniformly towards $\tau_{ij} = 1$ and, to a lesser degree, towards $\tau_{ij} = 2$.

This migration results in a nonlinear variation of σ_τ with respect to α that can be modeled in the following way: let's suppose that, far from the bifurcation, τ_{ij} is uniformly distributed in $[1, \tau_{\max}]$. Approaching the bifurcation, the lags τ_{ij} migrate towards small values, and we can write an ansatz for the distribution of lags as the superposition of a uniform and an exponential distribution:

$$p(\tau_{ij}) = f/\tau_{\max} + A\exp(-\beta\tau_{ij}), \tag{8}$$

where f, A and β depend on the bifurcation parameter, α. Given f and β, A can be calculated using the normalization condition $\sum p(\tau_{ij}) = 1$.

Using this equation, $\langle\tau\rangle$ and σ_τ can be computed as a function of f for a given β. As shown in Fig. 3 (solid lines), $\langle\tau\rangle$ decreases linearly with f, but σ_τ exhibits a local maximum. In Fig. 3 we also show the values of $\langle\tau\rangle$ and σ_τ (as dots colored according to the value of the bifurcation parameter α) and we estimate the value of f from the distribution of τ_{ij} for $\tau_{ij} > 10$, where the exponential term is negligible. A good agreement with Eq. (8) is evident, thus providing a simple interpretation of the variation of σ_τ that makes it a useful indicator of an approaching transcritical bifurcation.

4.3. Saddle-node bifurcation

In the LPF model presented in Section 3.2, when the amount of rainfall, R (bifurcation parameter), decreases below $R_c = 1.1$, a saddle-node bifurcation occurs which causes a collapse from a vegetated state ($B > 0$) to a desert state ($B = 0$). As in the previous case, close to the bifurcation, we see in Fig. 4 that σ_τ displays a maximum, while the other indicators vary monotonically.

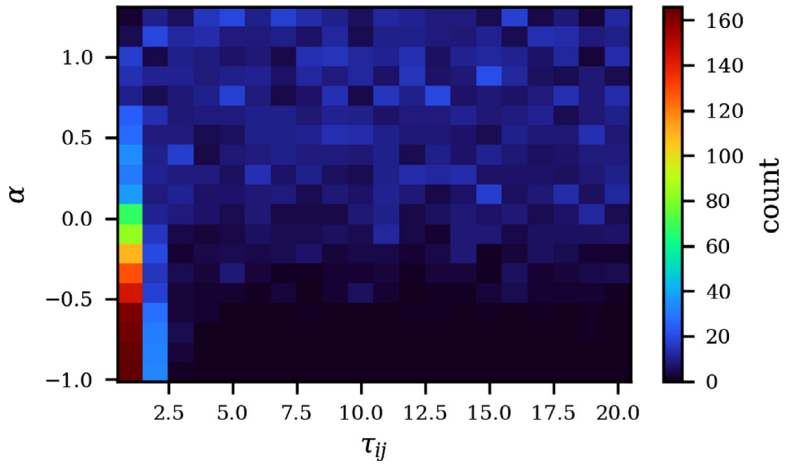

Fig. 2. Histogram of τ_{ij} values (in color code) as a function of the bifurcation parameter, α, for the scalar bistable 1D model.

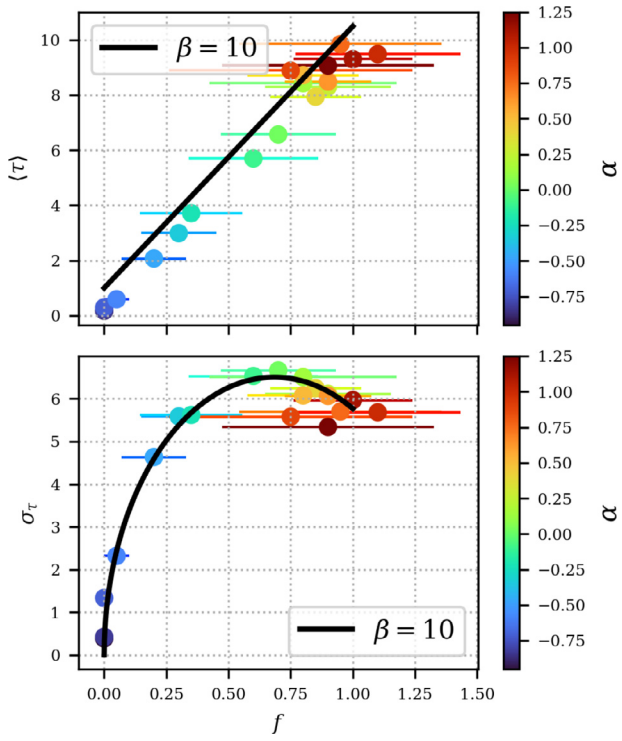

Fig. 3. Average, $\langle\tau\rangle$, and standard deviation, σ_τ, of the lag distribution as a function of the parameter f in Eq. (8), for the scalar bistable 1D model. The color code indicates the value of the bifurcation parameter, α, and the black line depicts the values predicted by Eq. (8) for $\beta = 10$. The horizontal bars represent the uncertainty on the estimation of f, that is estimated, from each histogram, as the median value of the frequency in the tail, and the standard deviation is used to measure of uncertainty of that estimate.

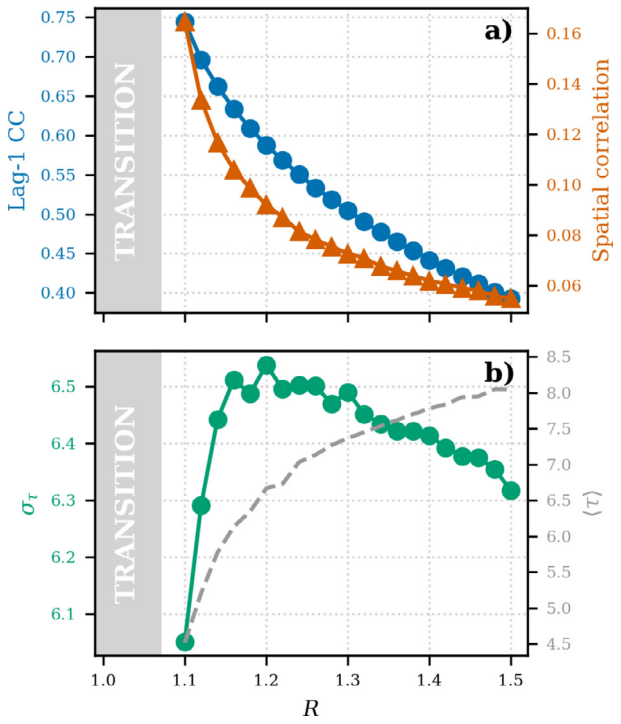

Fig. 4. Early warning indicators as a function of the bifurcation parameter, R, for the saddle-node bifurcation of the LPF model. (a) Lag-1 correlation and spatial correlation. (b) Average, $\langle\tau\rangle$, and standard deviation, σ_τ, of the distribution of lags that maximize the absolute value of the cross-correlation between first neighbors.

To confirm that the simple model for σ_τ presented previously also works here, we repeated the analysis. The behavior of σ_τ in function of the parameter f is depicted in Fig. 5. Also in this case, the behavior predicted by Eq. (8) fits the behavior of σ_τ computed from the biomass time series. As before, the parameter f was estimated from the distribution of τ_{ij} values for $\tau_{ij} > 10$, where the term $A\exp(-\beta\tau)$ is negligible.

4.4. Saddle-focus bifurcation

As shown in Table 1, the FHN model displays a variety of bifurcations. For appropriate parameters, the system has three fixed points, two stable and one unstable. When varying the bifurcation parameter I a saddle-focus bifurcation occurs, and the presence of noise sustains subthreshold oscillations around the stable fixed point. These oscillations dominate the dynamics and render the spatial correlation useless for predicting the approaching bifurcation (Fig. 6a). However, in Fig. 6b we can see that σ_τ varies considerably approaching the bifurcation. In this case, the increase is monotonous, lacking the turning point we have seen in the transcritical and saddle-node bifurcations.

4.5. Supercritical Hopf bifurcation

For appropriate parameters the FHN model exhibits a supercritical Hopf bifurcation, where a stable fixed point loses stability while a stable periodic orbit appears. As in the previous case,

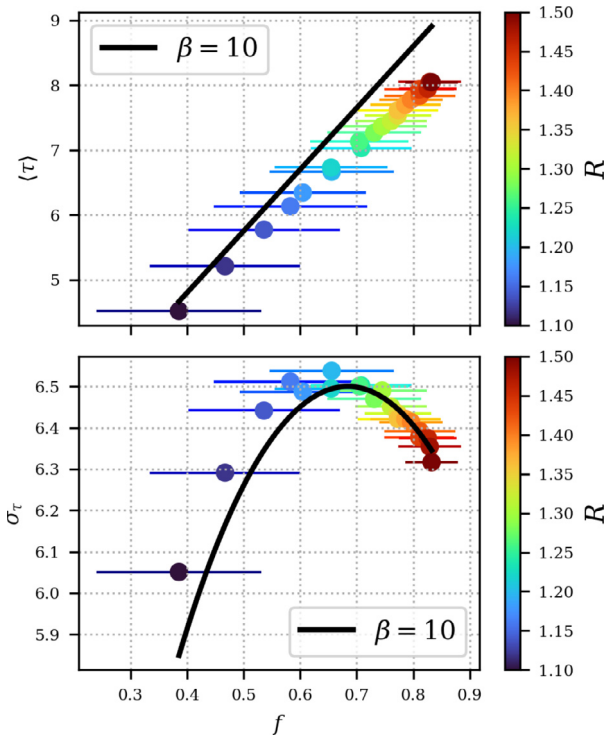

Fig. 5. Average, $\langle\tau\rangle$, and standard deviation, σ_τ, of the lag distribution as a function of the parameter f in Eq. (8), for the LPF model. The black line depicts the values predicted by Eq. (8) for $\beta = 10$.

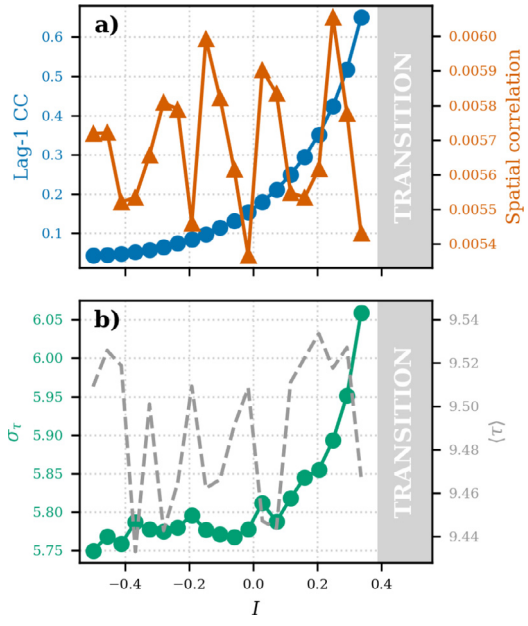

Fig. 6. Early warning indicators as a function of the bifurcation parameter I for the saddle-focus bifurcation of the FHN model. **(a)** Lag-1 correlation and spatial correlation. **(b)** average ($\langle\tau\rangle$) and standard deviation (σ_τ) of the lag distribution.

the eigenvalues are imaginary, thus producing subthreshold oscillations, but the spatial correlation increases in the proximity of the bifurcation (Fig. 7a). σ_τ displays again a maximum that provides the early warning for the transition (Fig. 7b).

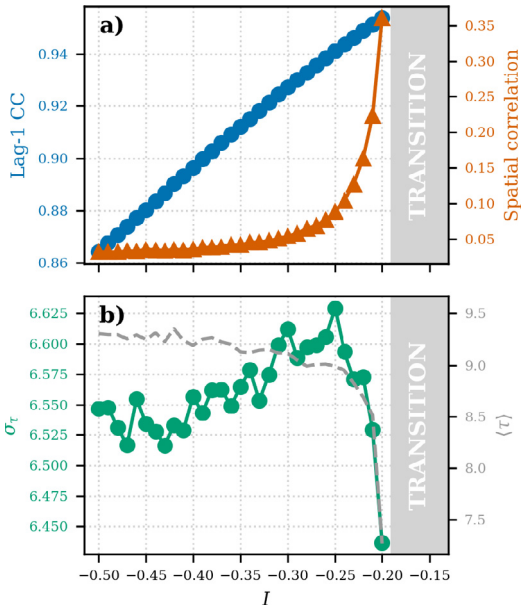

Fig. 7. As Fig. 6, but for the supercritical Hopf bifurcation.

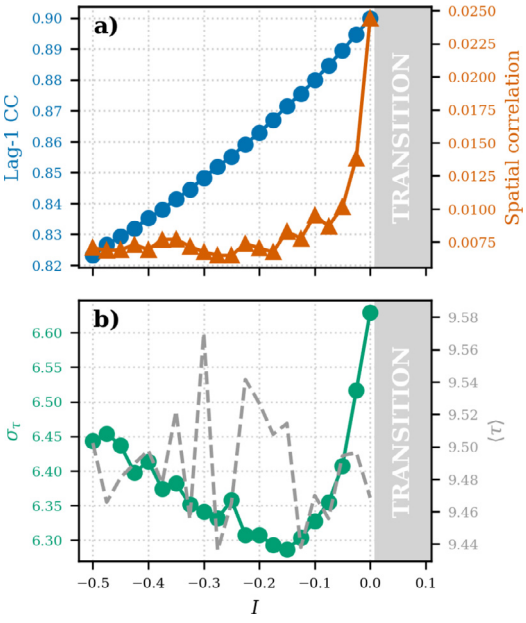

Fig. 8. As Fig. 6, but for the subcritical Hopf bifurcation.

4.6. Subcritical Hopf bifurcation

In the FHN model, for appropriate parameters, an unstable orbit and a stable fixed point coalesce giving rise to an unstable fixed point. The system loses stability and evolves towards a second, stable fixed point. The behavior of the classical indicators (Fig. 8a) is similar to the one seen in the supercritical bifurcation. However, the behavior of σ_τ is opposite: approaching the bifurcation σ_τ decreases and, when the bifurcation is close enough, it increases abruptly (Fig. 8b).

4.7. Global bifurcation

The spatial FHN model can also host several types of traveling waves [46]. In the case of the subcritical Hopf bifurcation, increasing one of the diffusion coefficients enables the propagation

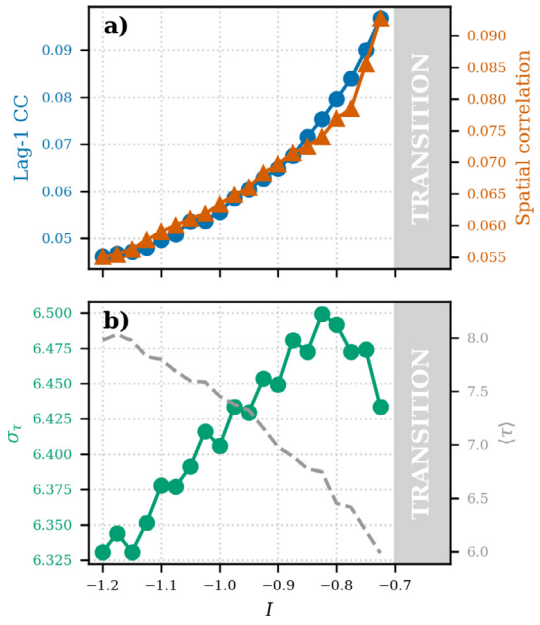

Fig. 9. As Fig. 6, but for the traveling waves instability.

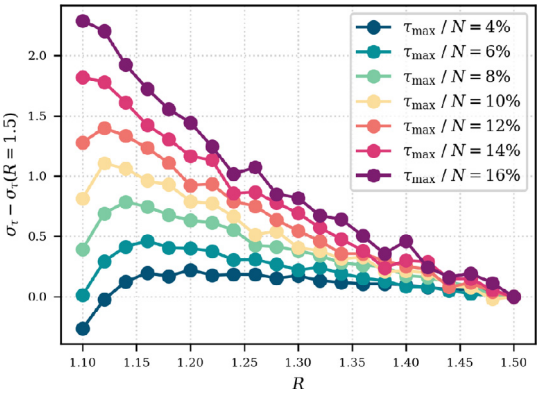

Fig. 10. Variation of σ_τ with respect to τ_{max}, for the LPF model. We see that if τ_{max} is too large the extreme point disappears.

of nonlinear waves. When crossing a threshold value of the bifurcation parameter, I, the presence of noise can excite a local pulse that starts traveling with a circular front. This happens when the system is not bistable yet, and the traveling waves are pulses. If I increases further up to the bistability, the traveling pulses turn into traveling fronts [46]. This instability is not due to a local bifurcation as the previous ones, but it is due to a global change in the phase-space structure (traveling pulses are due to the appearance of a heteroclinic orbit in the phase-space of the traveling waves' solution [47,48]). No eigenvalue crosses the imaginary axis, thus, there is no reason to expect critical slowing down. Nevertheless, the autocorrelation and spatial correlation increase, even if their absolute values are very modest (Fig. 9a). Importantly, σ_τ captures the approaching non-local bifurcation and drops right before (Fig. 9b). Again, we have a non-monotonic variation that reveals that the system is close to a loss of stability, although the loss is not due to a local bifurcation.

4.8. Sensitivity of σ_τ to the maximum lag

The value of the lag, τ_{ij}, that maximizes the absolute value of the cross-correlation between two time series, u_i and u_j, depends on one free parameter: the size of the interval $[1,\tau_{max}]$ within which we search for the maximum. This is the only free parameter of the indicator σ_τ that impacts its performance.

In the previous sections we kept fixed the maximum lag to 4% of the series length, N. Given $N = 500$, we have $\tau_{max} = 20$ time units (t.u.). In Fig. 10 we analyze, for the LPF model, the sensitivity of σ_τ when increasing τ_{max} up to 16% of N. We see that there is an upper limit above which the maximum of σ_τ disappears, or rather moves across the transition, making σ_τ no more useful than other indicators.

4.9. Continuous variation of the parameter

In previous sections we have tested the performance of σ_τ when the bifurcation parameter is varied in small steps, and here we test its performance when the parameter varies continuously. Specifically, we consider a linear variation and analyze the performance of σ_τ as a function of the rate of variation of the parameter and the size of the sliding window used to compute the cross correlation. To study the influence of the rate of variation of the parameter, we kept constant the duration of the interval $[1,\tau_{max}]$ with $\tau_{max} = 20$ t.u., while to study the influence of the size of the window we kept constant the relative duration of the interval: 4% of the size of the window used to compute the cross correlation. Results for the LPF model are presented in Figs. 11 and 12 respectively. We see that when the time window is small enough, such that the variation of the bifurcation parameter, R, is small, and when τ_{max} is not too small (in this case 10% performs well), then σ_τ reaches a maximum that is an indication of the upcoming bifurcation.

5. Conclusions

In summary, we have shown that the standard deviation of the distribution of lag times, σ_τ, is a robust indicator of an approaching bifurcation, not only in the context of a local bifurcation, but also, when a global bifurcation occurs.

The lag-1 autocorrelation consistently rises in response to an eigenvalue whose real part goes to zero but this rise may be

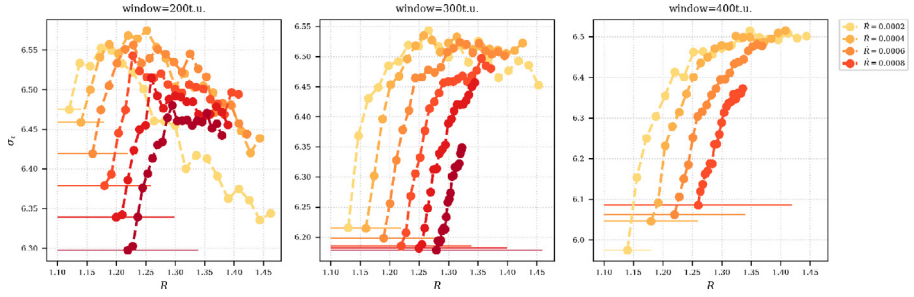

Fig. 11. σ_τ in function of the bifurcation parameter, R, for different rate of variation of R and for different window sizes used to compute σ_τ. Horizontal whiskers mark the range of variation of R in each time window. In this case, τ_{max} is always 20 t.u.

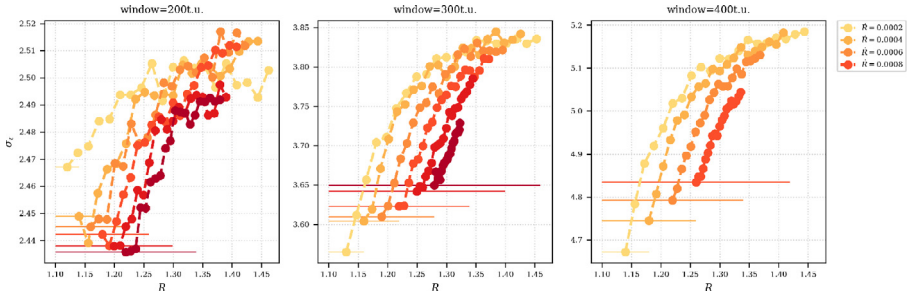

Fig. 12. σ_τ in function of the bifurcation parameter, R, for different rate of variation of R and for different window sizes used to compute σ_τ. Horizontal whiskers mark the range of variation of R in each time window. In this case, τ_{max} is always 4% of the window size.

monotonous and thus, not particularly informative. In contrast, when the system's spatial correlation increases, σ_τ displays a maximum that serves as an indication of the approaching bifurcation. When there is no increase in spatial correlation, σ_τ varies monotonically, and thus, it is as useful as the lag-1 autocorrelation. We have also proposed a simple model to explain the underlying origin of the maximum of σ_τ that serves as a warning of the approaching bifurcation.

When there are subthreshold oscillations before the bifurcation, as the bifurcation is approached, σ_τ displays a minimum, that also serves as early warning of the bifurcation. We interpret the minimum as due to the fact that the oscillations give rise to a local maximum of the cross-correlation at the oscillation period. This maximum creates a second peak in the distribution of the lags, increasing the lags variance.

More in general, we believe that the success of the indicator σ_τ relies on the fact that its calculation involves the analysis of lags within an interval of values, and therefore takes into account properties of the time series that may be linked to the changes happening in the phase space. Further analysis in this direction will be undertaken to advance our understanding of the performance of this new early warning indicator.

Declaration of Competing Interest

The authors declare that they have no known competing financial interests or personal relationships that could have appeared to influence the work reported in this paper.

Acknowledgments

This work was funded by the Spanish Ministerio de Ciencia, Innovación y Universidades (PGC2018-099443-B-I00) and the ICREA ACADEMIA program of Generalitat de Catalunya.

References

[1] Scheffer M, Carpenter S, Foley JA, Folke C, Walker B. Catastrophic shifts in ecosystems. Nature 2001;413(6856):591–6.
[2] Lenton TM. Early warning of climate tipping points. Nat Clim Change 2011;1(4):201–9.
[3] Thompson JMT, Sieber J. Predicting climate tipping as a noisy bifurcation: a review. Int J Bifurc Chaos 2011;21(02):399–423.
[4] Scheffer M, Carpenter SR, Lenton TM, Bascompte J, Brock W, Dakos V, de Koppel JV, de Leemput IAV, Levin SA, Nes EHV, et al. Anticipating critical transitions. Science 2012;338(6105):344–8.
[5] D'Souza RM, Gomez-Gardenes J, Nagler J, Arenas A. Explosive phenomena in complex networks. Adv Phys 2019;68:123–223.
[6] Ashwin P, Wieczorek S, Vitolo R, Cox P. Tipping points in open systems: bifurcation, noise-induced and rate-dependent examples in the climate system. Philos Trans R Soc A 2012;370(1962):1166–84.
[7] Vanselow A, Wieczorek S, Feudel U. When very slow is too fast–collapse of a predator-prey system. J Theor Biol 2019;479:64–72.
[8] Chen P, Chen E, Chen LN, Zhou XJ, Liu R. Detecting early-warning signals of influenza outbreak based on dynamic network marker. J Cell Mol Med 2019;23:395–404.
[9] Hastings A. Regime shifts in ecological systems can occur with no warning. Ecol Lett 2010;13:464–72.
[10] Buldyrev SV, Parshani R, Paul G, Stanley HE, Havlin S. Catastrophic cascade of failures in interdependent networks. Nature 2010;464:1025–8.
[11] Hughes TP, Linares C, Dakos V, van de Leemput IA, van Nes EH. Living dangerously on borrowed time during slow, unrecognized regime shifts. Trends Ecol Evol 2013;28(3):149–55.
[12] Jiang JJ, Hastings A, Lai YC. Harnessing tipping points in complex ecological networks. J R Soc Interface 2019;16:20190345.
[13] O'Keeffe P, Wieczorek S. Tipping phenomena and points of no return in ecosystems: beyond classical bifurcations. SIAM J Appl Dyn Syst 2020;19(4):2371–402.
[14] Ott E. Chaos in dynamical systems. Cambridge University Press; 2002.
[15] Carpenter SR, Brock WA. Rising variance: a leading indicator of ecological transition. Ecol Lett 2006;9:308–15.
[16] Guttal V, Jayaprakash C. Changing skewness: an early warning signal of regime shifts in ecosystems. Ecol Lett 2008;11:450–60.
[17] Andersen T, Carstensen J, Hernandez-Garcia E, Duarte CM. Ecological thresholds and regime shifts: approaches to identification. Trends Ecol Evol 2009;24(1):49–57.
[18] Dakos V, Carpenter SR, Brock WA, et al. Methods for detecting early warnings of critical transitions in time series illustrated using simulated ecological data. PLoS One 2012;7:41010.
[19] van de Leemput IA, et al. Critical slowing down as early warning for the onset and termination of depression. PNAS 2014;111(1):87–92.
[20] Wichers M, Groot PC, et al. Critical slowing down as a personalized early warning signal for depression. Psychother Psychosom 2016;85:114–16.
[21] Nazarimehr F, Jafari S, Golpayegani SMRH, Sprott JC. Can Lyapunov exponent predict critical transitions in biological systems? Nonlinear Dyn 2017;88:1493–500.
[22] Kuhlmann L, Lehnertz K, Richardson MP, Schelter B, Zaveri HP. Seizure prediction–ready for a new era. Nat Rev Neurol 2018;14(10):618–30.
[23] Rings T, von Wrede R, Lehnertz K. Precursors of seizures due to specific spatial-temporal modifications of evolving large-scale epileptic brain networks. Sci Rep 2019;9(1):10623.
[24] Peng XY, Zhao Y, Small M. Identification and prediction of bifurcation tipping points using complex networks based on quasi-isometric mapping. Phys A 2020;560:125108.
[25] Maturana MI, et al. Critical slowing down as a biomarker for seizure susceptibility. Nat Commun 2020;11(1):2172.
[26] Boettner C, Klinghammer G, Boers N, Westerhold T, Marwan N. Early-warning signals for cenozoic climate transitions. Quat Sci Rev 2021;270:107177.
[27] Boers N, Rypdal M. Critical slowing down suggests that the western greenland ice sheet is close to a tipping point. PNAS 2021;118. E2024192118
[28] He WP, Xie XQ, Mei Y, Wan SQ, Zhao SS. Decreasing predictability as a precursor indicator for abrupt climate change. Clim Dyn 2021;56:3899–908.
[29] Mandel P. Theoretical problems in cavity nonlinear optics, vol 21. Cambridge University Press; 2005.
[30] Tredicce JR, Lippi GL, Mandel P, Charasse B, Chevalier A, Picqué B. Critical slowing down at a bifurcation. Am J Phys 2004;72(6):799–809.
[31] Masoller C, Hong Y, Ayad S, Gustave F, Barland S, Pons AJ, et al. Quantifying sudden changes in dynamical systems using symbolic networks. New J Phys 2015;17(2):023068.
[32] Marconi M, Métayer C, Acquaviva A, Boyer JM, Gomel A, Quiniou T, Masoller C, Giudici M, Tredicce JR. Testing critical slowing down as a bifurcation indicator in a low-dissipation dynamical system. Phys Rev Lett 2020;125(13):134102.
[33] Guttal V, Jayaprakash C. Spatial variance and spatial skewness: leading indicators of regime shifts in spatial ecological systems. Theor Ecol 2009;2(1):3–12. doi:10.1007/s12080-008-0033-1.
[34] Dakos V, van Nes EH, Donangelo R, Fort H, Scheffer M. Spatial correlation as leading indicator of catastrophic shifts. Theor Ecol 2010;3(3):163–74.
[35] Mheen MVD, Dijkstra HA, Gozolchiani A, Toom MD, Feng Q, Kurths J, et al. Interaction network based early warning indicators for the atlantic moc collapse. Geophys Res Lett 2013;40(11):2714–19.
[36] Tirabassi G, Viebahn J, Dakos V, Dijkstra HA, Masoller C, Rietkerk M, et al. Interaction network based early-warning indicators of vegetation transitions. Ecol Complex 2014;19:148–57.

[37] Rodríguez-Méndez V, Eguíluz VMM, Hernández-García E, Ramasco JJ. Percolation-based precursors of transitions in extended systems. Sci Rep 2016;6(June):1–11. doi:10.1038/srep29552.
[38] Biggs R, Carpenter SR, Brock WA. Turning back from the brink: detecting an impending regime shift in time to avert it. PNAS 2009;106:18001.
[39] Boettiger C, Hastings A. Quantifying limits to detection of early warning for critical transitions. J R. Soc Interface 2012;9:2527–39.
[40] Ghanavati G, Hines PDH, Lakoba TI. Identifying useful statistical indicators of proximity to instability in stochastic power systems. Trans Power Syst 2016;31:1360–8.
[41] Wilkat T, Rings T, Lehnertz K. No evidence for critical slowing down prior to human epileptic seizures. Chaos 2019;29(9):091104.
[42] Quintero-Quiroz C, Torrent MC, Masoller C. State space reconstruction of spatially extended systems and of time delayed systems from the time series of a scalar variable. Chaos 2018;28(7):1–7.
[43] FitzHugh R. Impulses and physiological states in theoretical models of nerve membrane. Biophys J 1961;1(6):445–66.
[44] Nagumo J, Arimoto S, Yoshizawa S. An active pulse transmission line simulating nerve axon. Proc IRE 1962;50(10):2061–70.
[45] Purwins H-G, Bödeker HU, Liehr AW. Dissipative solitons in reaction-diffusion systems. In: Dissipative solitons. Springer; 2005. p. 267–308.
[46] Lindner B, García-Ojalvo J, Neiman A, Schimansky-Geier L. Effects of noise in excitable systems. Phys Rep 2004;392(6):321–424.
[47] Pauwelussen JP. Heteroclinic waves of the Fitzhugh–Nagumo equations. Math Biosci 1982;58(2):217–42.
[48] Cornwell P, Jones CK. On the existence and stability of fast traveling waves in a doubly diffusive Fitzhugh–Nagumo system. SIAM J Appl Dyn Syst 2018;17(1):754–87.